Novel method for the angular chirp compensation of passively CEP-stable few-cycle pulses

GIOVANNI CIRMI,[1,2,5,6] 🆔 HÜSEYIN ÇANKAYA,[1,2,5,7] 🆔 PETER KROGEN,[3] ANNE-LAURE CALENDRON,[1,2] 🆔 YI HUA,[1] BENOIT DEBORD,[4] FRÉDÉRIC GÉRÔME,[4] FETAH BENABID,[4] AND FRANZ X. KÄRTNER[1,2] 🆔

[1]*Center for Free Electron Laser Science (CFEL), Deutsches Elektronen-Synchrotron (DESY) & Department of Physics, University of Hamburg, Notkestraße 85, 22607 Hamburg, Germany*
[2]*The Hamburg Center for Ultrafast Imaging, Luruper Chaussee 149, 22761 Hamburg, Germany*
[3]*Department of Electrical Engineering and Computer Science and Research Laboratory of Electronics, Massachusetts Institute of Technology (MIT), Cambridge, Massachusetts 02139, USA*
[4]*GPPMM Group, Xlim Research Institute, UMR 7252 CNRS, University of Limoges, Limoges, France*
[5]*These authors contributed equally*
[6]*giovanni.cirmi@desy.de*
[7]*huseyin.cankaya@cfel.de*

Abstract: We demonstrate a novel, energy-efficient, cost-effective simple method for seeding CEP-stable OPCPAs. We couple the CEP-stable idler of a broadband OPCPA into a hollow core Kagome fiber thus compensating for the angular chirp. We obtain either relatively narrow bandwidths with ~36% coupling efficiency or quarter-octave spanning bandwidths with ~2.2% coupling efficiency. We demonstrate spectral compressibility, good beam quality and CEP stability. Our source is an ideal seed for high-energy, high-average power, CEP-stable few-cycle OPCPA pulses around 2 μm, which can drive the generation of coherent soft X-ray radiation in the water window spectral region via HHG.

1. Introduction

The generation of coherent water window (WW) radiation (282-533 eV) is one of the most explored research topics of the ultrafast optics community in the latest years [1–8]. WW sources allow for a new regime of spectroscopy with attosecond resolution of biological samples, because this part of the electromagnetic spectrum is transmitted by water and absorbed by carbon.

The present method to generate WW radiation consists in driving high harmonic generation (HHG) with infrared pulses. From several theoretical and experimental papers, it turns out that the spectral region around 2 μm is a good compromise between HHG efficiency and cut-off extension to drive the production of coherent WW radiation [9]. The driver pulses ideally need to have ~mJ energies to drive enough HHG in the WW to be used in experiments, broad bandwidth and short duration to produce isolated attosecond pulses (IAPs) and carrier-envelope phase (CEP) stability to generate pulse-to-pulse reproducible IAPs. In addition, the latest high-power laser developments have shown that it is possible to produce very high average power ~ps pump pulses at 1 μm [10–14]. Therefore, a good candidate to drive HHG in the WW is a 1-μm-pumped optical parametric chirped pulse amplifier (OPCPA) at 2 μm central wavelength. Such parametric sources can reach few-optical cycle duration and ~mJ energies. When combined either with spectral broadening stages, in hollow core photonic crystal fibers (HCPCF) or Herriott cells, or with attosecond gating techniques, or in a parametric synthesis configuration, these sources can drive IAPs in the WW spectral region.

The CEP stability of the driver, allowing for pulse-to-pulse reproducibility of IAPs, can be achieved either deriving the optical setup from an actively stabilized laser [15,16] or passively through difference frequency generation (DFG) between pulses coming from the same laser [17]. In the case of the OPCPA, or optical parametric amplifier (OPA), the idler pulses are the DFG between pump and signal pulses, so they are passively CEP-stabilized even if they are derived from non-CEP-stable lasers.

Using the CEP-stable idler of an OP(CP)A as a seed for successive OP(CP)A stages seems to be a straightforward way to achieve high-energy CEP-stable pulses, but we will discuss the accompanying hurdle. The broadest-bandwidth achievable from an OPCPA at 2 µm with pump at 1 µm is in a degenerate OPCPA (DOPA) configuration in β-barium borate (BBO) crystal or in similar crystals with type I phase matching. In this case the spectra of signal and idler are both quarter-octave spanning around 2 µm. The polarizations of signal and idler are identical, and opposite to the pump polarization. If we use a strictly collinear configuration of pump and signal, at the output it is impossible to distinguish the CEP-unstable signal pulses from the CEP-stable idler pulses, since they have the same wavelength range, the same polarization and the same direction of propagation. Therefore, a strictly collinear DOPA cannot be used for seeding successive CEP-stable amplification stages. A slight non-collinear angle (0-2°) between pump and signal does not drastically change the phase matching bandwidth, but it allows a spatial discrimination between idler and signal. It would be in principle possible to use a slightly non-collinear DOPA as a seed for successive stages, but the angular dispersion of the idler due to the different phase matching condition for each of its wavelengths makes this task very difficult; a correction of the spatial chirp is then required. There have been a number of proposals in the past to solve this problem [18] and to generate a CEP-stable few-cycle seed for OP(CP)As. One of them consists in compensating the idler angular chirp with gratings and deformable mirrors [19]. It is an efficient technique and shows good performances, but it is costly and complex. Another scheme [20] consists in using a narrowband collinear [21] or slightly non-collinear OPA [22] whose CEP-stable idler has none or negligible angular chirp compared to its natural divergence, and whose frequency is well separated from the signal. The idler, or its second harmonic, is used to pump a CEP-stable white light generation (WLG) stage in bulk materials. This scheme has shown to be very successful and is being used in several optical parametric synthesizers, because it can produce a CEP-stable seed over multiple octaves [23,24]. Its drawback is the low efficiency, since the energy of the OPA generates the supercontinuum with $\sim 10^{-3}$ efficiency, and the total efficiency from the laser is $\sim 10^{-5}$ [24].

Here, we introduce a novel simple and efficient all-optical scheme for the generation of CEP-stable pulses, which can be used to seed successive amplification stages. We also utilized our concept in a proof-of-principle experiment and showed good performance. The method consists in focusing the light of broadband slightly non-collinear DOPA, whose idler is CEP-stable but angularly dispersed, into a hollow core photonic crystal fiber (HCPCF) [25]. The inhibited-coupling HCPCF, which can easily handle hundreds-µJ pulse energies thanks to very low optical power overlap between core mode and silica cladding [26], homogenizes the wave-vector directions of the different idler wavelengths coupled into the fiber. This method is similar to the technique used for homogenizing diode lasers [27].

The laser for all our experiments was a home-built Yb:KYW regenerative amplifier [28] already used for the CEP-stable front-end in an Yb based optical parametric synthesizer [24]. It produces 5.4-mJ, 650-fs pulses at 1030 nm with 1 kHz repetition rate. We pumped and seeded a DOPA centered at 2 µm, and focused the idler into a HCPCF, in particular an inhibited coupling Kagome fiber [29] used in the linear regime. At the output of the fiber, the CEP-stable broadband idler has a well-defined propagation direction and no detectable angular chirp, and can be directly utilized as a seed for successive DOPA stages.

We believe that our technique is simpler and more effective in angular chirp compensation than other techniques based on gratings and deformable mirrors [18,19,30] and 2-3 orders of magnitude more energy-efficient than the sequence of a narrowband OPA and a WLG stage [24].

2. 'Narrowband' OPA

In a first experiment (setup scheme in Fig. 1), we used 308 μJ of the total pump laser energy at 1 kHz repetition rate [31]. We generated the seed by focusing a 13-μJ fraction of the driving laser output into a 10-mm-long YAG crystal. The WLG seed was amplified in two consecutive DOPA stages with type-I 4-mm-long BBO crystals cut at 21.8°. In the first stage, the pump energy was 73 μJ. In the second stage, the pump energy was 217 μJ and the pump intensity was ~130 GW/cm^2. The signal output energy of the first DOPA stage was ~240 nJ, the signal and idler energies after the second stage were 10.6 μJ each. The full width at half maximum (FWHM) of the spectrum was relatively narrowband (80 nm). We imaged the idler into the Kagome HCPCF with a 3.5:1 imaging system with 1 lens (f = 75 mm, ~34.5 cm between OPA output and lens, ~10 cm between lens and fiber). The fiber was in air, only 22-cm long in order to avoid unwanted nonlinear effects, with 7-core cells and 63-μm core diameter. The numerical aperture (NA) was ~0.018 [29], therefore its acceptance angle was ~2°. The output energy after the fiber was 3.8 μJ, so the coupling efficiency was 36%. We attribute the losses to the beam size at the input, which was larger than the fiber core diameter. The overall efficiency from the laser energy to the OPA output was 1.2×10^{-2}. We measured the pump beam diameter at 1/e^2 at the second stage as ~800 μm. Assuming that the idler had a similar size at the crystal, the beam size at the fiber input would be ~230 μm. The beam at the output of the fiber was collimated via a converging lens with 15 mm focal length. To check the residual angular dispersion, we propagated the beam few meters and then scanned over the beam profile via a multimode fiber coupled spectrometer. The beam diameter at 1/e^2 was >1 mm, well above the 105 μm core size. We measured the spectrum at several positions of the beam by moving the fiber horizontally and vertically, and diagonally. The measured spectrum at every position of the fiber relative to the beam was the same, which means that there was no residual angular chirp after the fiber output.
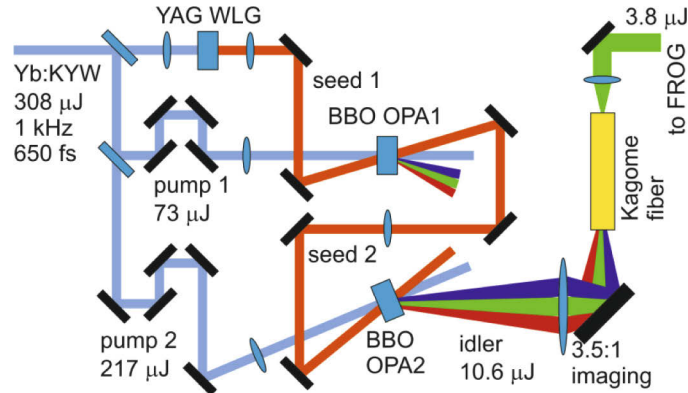

Fig. 1. Optical layout of the 'narrowband' CEP-stable seed generator.

We verified that the fiber did not introduce an oscillatory spectral phase which would not be difficult to compensate. To this aim, we measured the temporal profile of the pulses at the output of the fiber via second harmonic generation frequency resolved optical gating (SHG FROG). The spectrum supports pulses with a 32 fs duration when transform limited. We measured a pulse with 65 fs duration. The retrieved spectral phase was regular and smooth, and we expect the pulses to be compressible with standard dispersion management techniques (Fig. 2).
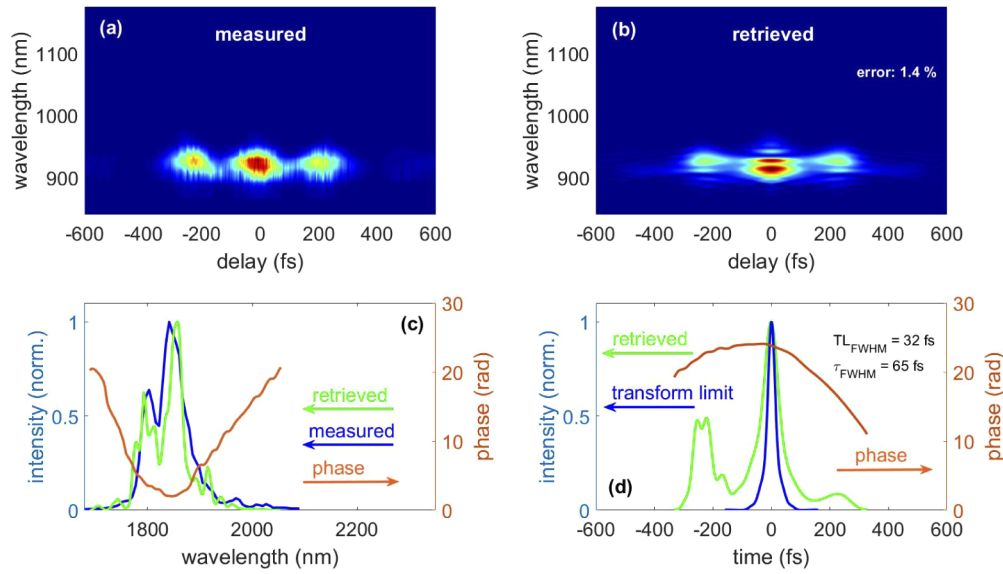
Fig. 2. Measured (a) and retrieved (b) FROG traces of the 'narrowband' HCPCF output; (c) measured (blue) and retrieved (green) spectral intensity, retrieved spectral phase (orange); (d) transform limit of the measured spectrum (blue), retrieved temporal intensity (green) and temporal phase (orange). For ease of comparison, the axes are the same as in Fig. 5. The reconstruction error is 1.4%.
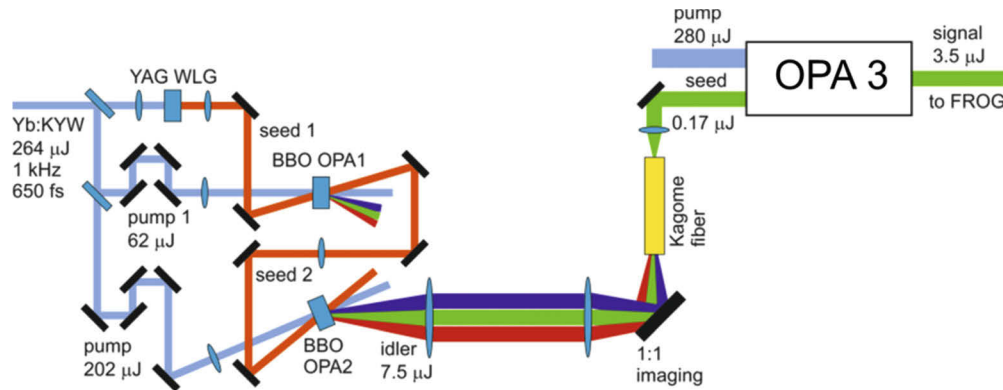

Fig. 3. Optical layout of the broadband CEP-stable seed generator.

3. Broadband OPA

After the experiment described above, we optimized the spectral content of the OPAs by adjusting the spectral content of the WLG seed and the phase matching angle, but not the pump-seed non-collinear angle. We estimate that the angular chirp may have approximately quadrupled. We coupled the OPA output into the fiber. Besides not being able to couple the whole bandwidth to the fundamental mode of the fiber due to the fiber acceptance angle, we measured a fringed spectrum as well as a fringed beam profile at the output. We attributed this problem to the excitation of higher order modes of the fiber, which beat with each other and cause the observed modulations. We then minimized the OPA angular chirp by minimizing the pump-seed external angle to ~1.6° at the second stage, and measured a ~1.8° external angular chirp. To measure

the angular chirp, we placed a multimode fiber (core size 105 μm) coupled to a spectrometer at ~81 cm from the OPA output and measured the spectrum at different positions along the idler beam. We considered as limits of the spectrum the short and long wavelengths whose maximum is as high as 4% of the global maximum of the spectrum at the center idler position. We used 62 μJ and 202 μJ pump power in the first and in the second stage. The pump intensity was ~120 GW/cm^2 at the second stage. A schematic of the setup is shown in Fig. 3.

We obtained a spectrum spanning from ~1.8 to 2.3 μm (340 nm FWHM) with 7.5 μJ energy. In this configuration, coupling into the Kagome fiber filtered out some idler spectral components at 1.75-1.8 μm and 2.3 to 2.35 μm. In addition, we modified the imaging setup into a 1:1 4-*f* imaging scheme (*f* = 100 mm). In this way, we matched the angular chirp to the 2° acceptance angle of the fiber, and were able to avoid spectral and spatial fringes. The drawback was the reduction in coupling efficiency to 2.2%, with ~170 nJ output energy. We attribute this loss in efficiency to the ~3.5 times bigger beam profile than in the previous experiment due to the different imaging configuration (~800 μm pump beam size). The overall efficiency from the laser to the fiber output was 6.4×10^{-4}. Figure 4(a) shows the good quality of the spatial profiles of
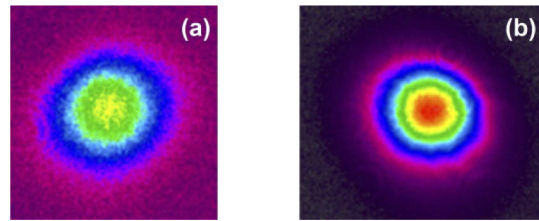

Fig. 4. Beam profile at (a) the output of the Kagome fiber for the broadband case, and (b) the output of the third broadband DOPA stage.
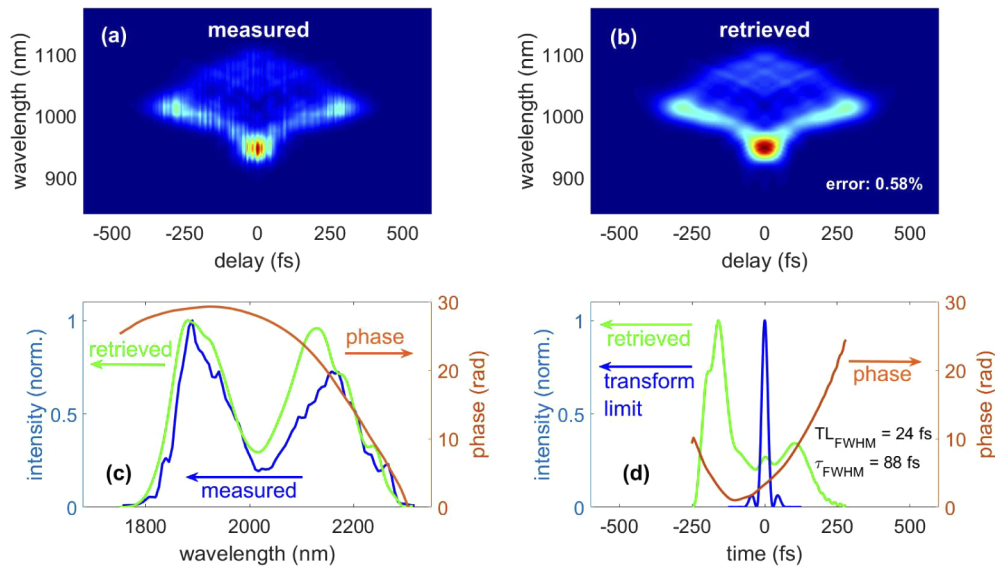

Fig. 5. Measured (a) and retrieved (b) FROG traces of the broadband third DOPA stage; (c) measured (blue) and retrieved (green) spectral intensity, retrieved spectral phase (orange); (d) transform limit of the measured spectrum (blue), retrieved temporal intensity (green) and temporal phase (orange). For ease of comparison, the axes are the same as Fig. 2. The reconstruction error is 0.58%.

the beam after the Kagome fiber (>1 mm beam diameter at $1/e^2$). Also in this case, we could not detect any residual angular chirp at the fiber output, by using the same procedure explained in section 2 for the narrowband case. We collimated the beam with the same $f = 15$ mm lens as before, and further amplified it in another 4-mm-long BBO crystal cut at 21.8° with 280 µJ pump energy. We obtained an amplified signal with 3.5-µJ energy and an excellent output signal beam profile, as shown in Fig. 4(b).

We measured the pulse with SHG-FROG and again retrieved a very smooth spectral phase which we expect to be compressible with standard techniques (Fig. 5). We think that the fringes along the time axis may be due to ~5% energy instabilities. The FWHM transform limit duration is 24 fs, and the measured FWHM duration is 88 fs. The setup did not show significant short- or long-term instability in energy and pointing.

4. CEP stability of the broadband OPA and perspectives

We characterized the passive CEP stability of the OPA output via $f-2f$ measurements. We split the pulse into 2 parts, produced supercontinuum via WLG in a 3-mm thick YAG plate and SHG in a 0.7-mm long BBO crystal, rotated the SHG polarization with a half waveplate and recombined the 2 branches in a spectrometer. We observed a good CEP stability, with 395 mrad rms fluctuations over 20 seconds (20 ms integration time, 20 shots per spectrum), as shown in Fig. 6. The $f-2f$ measurement shows the validity of the concept for the generation of a CEP-stable seed.
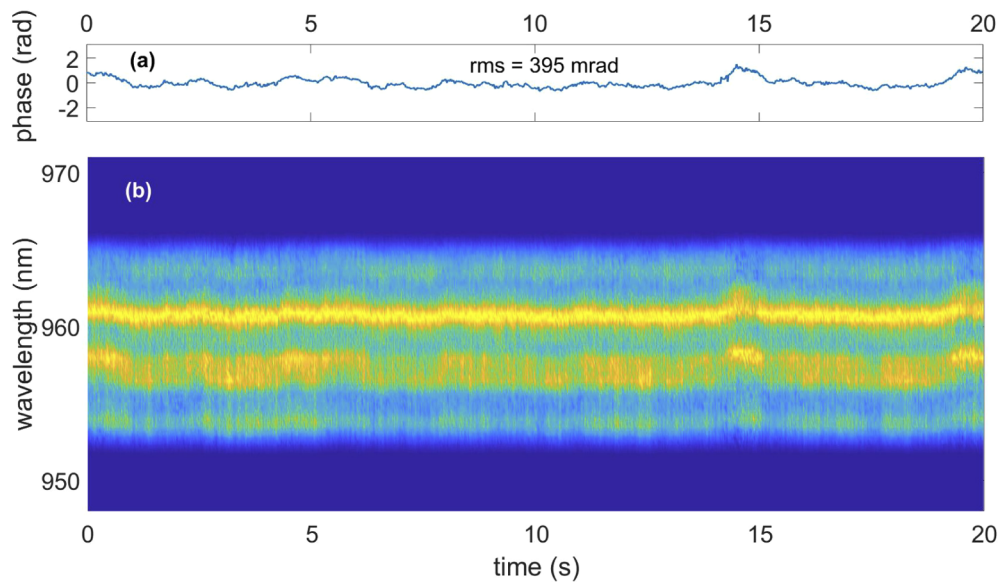

Fig. 6. The $f-2f$ of the broadband third stage DOPA output shows a CEP stability with rms = 395 mrad measured over 20 seconds, with 20 ms integration time (20 shots per spectrum). (a) CEP vs. time; (b) $f-2f$ spectrogram vs. time.

In addition, the setup could be improved by coupling the idler of the first OPA stage, and not of the second stage, into the Kagome fiber. This would reduce the CEP instability, due to the shorter path length difference between pump and signal [21], and it would also improve the coupling efficiency into the Kagome fiber, as explained in the following. In the second stage, due to the higher pump intensity, we used a big beam size (~800 µm) to avoid crystal damage and unwanted nonlinearities. When focusing the idler beam into the fiber, we have to compromise between

beam size in the focus and angular chirp. A big beam size at the crystal output can be focused to a small beam but with high angular chirp exceeding the fiber acceptance angle. Coupling the first stage instead of the second would be therefore more efficient, because of the smaller beam size of the first stage output in respect to the second. The disadvantage would be the difficulty of coupling a signal with ~100 times lower signal levels into the fiber, due to the difficulty of detection at 2 µm wavelength. Going to higher repetition rate (~10 kHz) would mitigate this issue.

5. Conclusion

We conceived and experimentally demonstrated a novel all-optical method for the generation of CEP-stable broadband pulses. The method consists in coupling the passively-CEP-stable idler of a broadband OP(CP)A into a HCPCF, used to correct for the angular chirp of the idler. It is simple, cost-effective, and energy-efficient if compared with other methods. We showed the feasibility and quality of this approach in terms of beam profile, spectral content, compressibility of the spectral phase, CEP stability in a proof-of-principle experiment. Several planned changes can improve the performances of our experimental apparatus: enclosing the setup, minimizing the beam path, coupling the first instead of the second stage into the fiber, further reducing the angular chirp, optimizing the design of the imaging system for better coupling efficiency. The generated CEP-stable pulses, being centered at 2-µm wavelength, can be used to seed high energy OPCPAs pumped by 1-µm Yb lasers. The OPCPAs can reach mJ-level energies, watts or even tens of watt average power, few-optical-cycle pulse durations. In combination with spectral broadening techniques, they are the ideal driver for the production of reproducible IAPs in the WW spectral region via HHG.

References

1. G. J. Stein, P. D. Keathley, P. Krogen, H. Liang, J. P. Siqueira, C.-L. Chang, C.-J. Lai, K.-H. Hong, G. M. Laurent, and F. X. Kärtner, "Water-window soft x-ray high-harmonic generation up to the nitrogen K-edge driven by a kHz, 2.1 µm OPCPA source," J. Phys. B: At. Mol. Opt. Phys. **49**(15), 155601 (2016).
2. S. M. Teichmann, F. Silva, S. L. Cousin, M. Hemmer, and J. Biegert, "0.5-keV Soft X-ray attosecond continua," Nat. Commun. **7**(1), 11493 (2016).
3. J. Li, X. Ren, Y. Yin, K. Zhao, A. Chew, Y. Cheng, E. Cunningham, Y. Wang, S. Hu, Y. Wu, M. Chini, and Z. Chang, "53-attosecond X-ray pulses reach the carbon K-edge," Nat. Commun. **8**(1), 186 (2017).
4. C. Schmidt, Y. Pertot, T. Balciunas, K. Zinchenko, M. Matthews, H. J. Wörner, and J.-P. Wolf, "High-order harmonic source spanning up to the oxygen K-edge based on filamentation pulse compression," Opt. Express **26**(9), 11834–11842 (2018).
5. D. Popmintchev, B. R. Galloway, M.-C. Chen, F. Dollar, C. A. Mancuso, A. Hankla, L. Miaja-Avila, G. O'Neil, J. M. Shaw, G. Fan, S. Ališauskas, G. Andriukaitis, T. Balčiunas, O. D. Mücke, A. Pugzlys, A. Baltuška, H. C. Kapteyn, T. Popmintchev, and M. M. Murnane, "Near- and Extended-Edge X-Ray-Absorption Fine-Structure Spectroscopy Using Ultrafast Coherent High-Order Harmonic Supercontinua," Phys. Rev. Lett. **120**(9), 093002 (2018).
6. V. Cardin, B. E. Schmidt, N. Thiré, S. Beaulieu, V. Wanie, M. Negro, C. Vozzi, V. Tosa, and F. Légaré, "Self-channelled high harmonic generation of water window soft x-rays," J. Phys. B: At. Mol. Opt. Phys. **51**(17), 174004 (2018).
7. A. S. Johnson, D. R. Austin, D. A. Wood, C. Brahms, A. Gregory, K. B. Holzner, S. Jarosch, E. W. Larsen, S. Parker, C. S. Strüber, P. Ye, J. W. G. Tisch, and J. P. Marangos, "High-flux soft x-ray harmonic generation from ionization-shaped few-cycle laser pulses," Sci. Adv. **4**(5), eaar3761 (2018).

8. C. Kleine, M. Ekimova, G. Goldsztejn, S. Raabe, C. Strüber, J. Ludwig, S. Yarlagadda, S. Eisebitt, M. J. J. Vrakking, T. Elsaesser, E. T. J. Nibbering, and A. Rouzeé, "Soft X-ray Absorption Spectroscopy of Aqueous Solutions Using a Table-Top Femtosecond Soft X-ray Source," J. Phys. Chem. Lett. **10**(1), 52–58 (2019).

9. T. Popmintchev, M.-C. Chen, A. Bahabad, M. Gerrity, P. Sidorenko, O. Cohen, I. P. Christov, M. M. Murnane, and H. C. Kapteyn, "Phase matching of high harmonic generation in the soft and hard X-ray regions of the spectrum," Proc. Natl. Acad. Sci. **106**(26), 10516–10521 (2009).

10. T. Nubbemeyer, M. Kaumanns, M. Ueffing, M. Gorjan, A. Alismail, H. Fattahi, J. Brons, O. Pronin, H. G. Barros, Z. Major, T. Metzger, D. Sutter, and F. Krausz, "1 kW, 200 mJ picosecond thin-disk laser system," Opt. Lett. **42**(7), 1381–1384 (2017).

11. C. Baumgarten, M. Pedicone, H. Bravo, H. Wang, L. Yin, C. S. Menoni, J. J. Rocca, and B. A. Reagan, "1 J, 0.5 kHz repetition rate picosecond laser," Opt. Lett. **41**(14), 3339–3342 (2016).

12. F. Beier, C. Hupel, S. Kuhn, S. Hein, J. Nold, F. Proske, B. Sattler, A. Liem, C. Jauregui, J. Limpert, N. Haarlammert, T. Schreiber, R. Eberhardt, and A. Tünnermann, "Single mode 4.3 kW output power from a diode-pumped Yb-doped fiber amplifier," Opt. Express **25**(13), 14892–14899 (2017).

13. M. Müller, M. Kienel, A. Klenke, T. Gottschall, E. Shestaev, M. Plötner, J. Limpert, and A. Tünnermann, "1 kW 1 mJ eight-channel ultrafast fiber laser," Opt. Lett. **41**(15), 3439–3442 (2016).

14. M. Kienel, M. Müller, A. Klenke, J. Limpert, and A. Tünnermann, "12 mJ kW-class ultrafast fiber laser system using multidimensional coherent pulse addition," Opt. Lett. **41**(14), 3343–3346 (2016).

15. T. Balčiūnas, O. D. Mücke, P. Mišeikis, G. Andriukaitis, A. Pugžlys, L. Giniūnas, R. Danielius, R. Holzwarth, and A. Baltuška, "Carrier envelope phase stabilization of a Yb:KGW laser amplifier," Opt. Lett. **36**(16), 3242–3244 (2011).

16. T. Balčiūnas, T. Flöry, A. Baltuška, T. Stanislauskas, R. Antipenkov, A. Varanavičius, and G. Steinmeyer, "Direct carrier-envelope phase control of an amplified laser system," Opt. Lett. **39**(6), 1669–1672 (2014).

17. A. Baltuška, T. Fuji, and T. Kobayashi, "Controlling the Carrier-Envelope Phase of Ultrashort Light Pulses with Optical Parametric Amplifiers," Phys. Rev. Lett. **88**(13), 133901 (2002).

18. S.-W. Huang, J. Moses, and F. X. Kärtner, "Broadband noncollinear optical parametric amplification without angularly dispersed idler," Opt. Lett. **37**(14), 2796–2798 (2012).

19. T.-J. Wang, Z. Major, I. Ahmad, S. A. Trushin, F. Krausz, and S. Karsch, "Ultra-broadband near-infrared pulse generation by noncollinear OPA with angular dispersion compensation," Appl. Phys. B **100**(1), 207–214 (2010).

20. G. Cirmi, C. Manzoni, D. Brida, S. De Silvestri, and G. Cerullo, "Carrier-envelope phase stable, few-optical-cycle pulses tunable from visible to near IR," J. Opt. Soc. Am. B **25**(7), B62–B69 (2008).

21. G. M. Rossi, L. Wang, R. E. Mainz, H. Çankaya, F. X. Kärtner, and G. Cirmi, "CEP dependence of Signal and Idler upon Pump-Seed synchronization in optical parametric amplifiers," Opt. Lett. **43**(2), 178–181 (2018).

22. C. Manzoni, D. Polli, G. Cirmi, D. Brida, S. De Silvestri, and G. Cerullo, "Tunable few-optical-cycle pulses with passive carrier-envelope phase stabilization from an optical parametric amplifier," Appl. Phys. Lett. **90**(17), 171111 (2007).

23. O. D. Mucke, S. Fang, G. Cirmi, G. M. Rossi, S.-H. Chia, H. Ye, Y. Yang, R. Mainz, C. Manzoni, P. Farinello, G. Cerullo, and F. X. Kartner, "Toward Waveform Nonlinear Optics Using Multimillijoule Sub-Cycle Waveform Synthesizers," IEEE J. Sel. Top. Quantum Electron. **21**(5), 1–12 (2015).

24. H. Çankaya, A.-L. Calendron, C. Zhou, S.-H. Chia, O. D. Mücke, G. Cirmi, and F. X. Kärtner, "40-μJ passively CEP-stable seed source for ytterbium-based high-energy optical waveform synthesizers," Opt. Express **24**(22), 25169–25180 (2016).

25. B. Debord, F. Amrani, L. Vincetti, F. Gérôme, and F. Benabid, "Hollow-Core Fiber Technology: The Rising of Gas Photonics," Fibers **7**(2), 16 (2019).

26. B. Debord, M. Alharbi, L. Vincetti, A. Husakou, C. Fourcade-Dutin, C. Hoenninger, E. Mottay, F. Gérôme, and F. Benabid, "Multi-meter fiber-delivery and pulse self-compression of milli-Joule femtosecond laser and fiber-aided laser-micromachining," Opt. Express **22**(9), 10735–10746 (2014).

27. M. Traub, H.-D. Hoffmann, H.-D. Plum, K. Wieching, P. Loosen, and R. Poprawe, "Homogenization of high power diode laser beams for pumping and direct applications," Proc. SPIE **6104**, 61040Q (2006).

28. A.-L. Calendron, H. Çankaya, and F. X. Kärtner, "High-energy kHz Yb:KYW dual-crystal regenerative amplifier," Opt. Express **22**(20), 24752–24762 (2014).

29. K. Murari, G. J. Stein, H. Cankaya, B. Debord, F. Gérôme, G. Cirmi, O. D. Mücke, P. Li, A. Ruehl, I. Hartl, K.-H. Hong, F. Benabid, and F. X. Kärtner, "Kagome-fiber-based pulse compression of mid-infrared picosecond pulses from a Ho:YLF amplifier," Optica **3**(8), 816–822 (2016).

30. K. Okamura and T. Kobayashi, "Octave-spanning carrier-envelope phase stabilized visible pulse with sub-3-fs pulse duration," Opt. Lett. **36**(2), 226–228 (2011).

31. G. Cirmi, H Cankaya, P. Krogen, A.-L. Calendron, Y. Hua, B. Debord, F. Gerome, F. Benabid, and F. X. Kärtner, "Novel method for CEP-stable seeding of few-cycle OPCPAs," *talk AM2A.3 at Advanced Solid State Lasers Conference*, Vienna (2019).